Interfacial scattering effect on anisotropic magnetoresistance and anomalous Hall effect in Ta/Fe multilayers

Qiang Zhang, Junwei Zhang, Yuelei Zhao, Yan Wen, Peng Li, Senfu Zhang, Xin He, Junli Zhang, and Xixiang Zhang

Citation: AIP Advances **8**, 055813 (2018);
View online: https://doi.org/10.1063/1.5006355
View Table of Contents: http://aip.scitation.org/toc/adv/8/5
Published by the American Institute of Physics

Interfacial scattering effect on anisotropic magnetoresistance and anomalous Hall effect in Ta/Fe multilayers

Qiang Zhang, Junwei Zhang, Yuelei Zhao, Yan Wen, Peng Li, Senfu Zhang, Xin He, Junli Zhang, and Xixiang Zhang[a]
Physical Science and Engineering Division (PSE), King Abdullah University of Science and Technology (KAUST), Thuwal 23955–6900, Saudi Arabia

(Presented 10 November 2017; received 25 September 2017; accepted 8 November 2017; published online 26 December 2017)

The effect of interfacial scattering on anisotropic magnetoresistance (AMR) and anomalous Hall effect (AHE) was studied in the $(Ta_{\frac{12}{n}}/Fe_{\frac{36}{n}})_n$ multilayers, where the numbers give the thickness in nanometer and n is an integer from 1 to 12. The multilayer structure has been confirmed by the XRR spectra and STEM images of cross-sections. The magneto-transport properties were measured by four-point probe method in Hall bar shaped samples in the temperature range of 5 – 300 K. The AMR increases with n, which could be ascribed to the interfacial spin-orbit scattering. At 5 K, the longitudinal resistivity (ρ_{xx}) increases by 6.4 times and the anomalous Hall resistivity (ρ_{AHE}) increases by 49.4 times from n =1 to n =12, indicative of the interfacial scattering effect. The skew-scattering, side-jump and intrinsic contributions to the AHE were separated successfully. As n increases from 1 to 12, the intrinsic contribution decreases because of the decaying crystallinity or finite size effect and the intrinsic contribution dominated the AHE for all samples. The side jump changes from negative to positive because the interfacial scattering and intralayer scattering in Fe layers both contribute to side jump in the AHE but with opposite sign.
https://doi.org/10.1063/1.5006355

I. INTRODUCTION

The anomalous Hall effect (AHE) has been intensively studied in magnetic materials due to its controversial mechanisms[1–6] and promising applications.[7] It is generally accepted that the intrinsic and extrinsic mechanisms, related to spin-orbit coupling (SOC), are responsible for the AHE. The intrinsic mechanism[1–4] originates from the Berry curvature of the occupied Bloch state. The extrinsic mechanisms, arising from impurity scattering, include two contributions, skew scattering[5] and side jump.[6] Theories also suggested the scaling relations[2,5,6] between anomalous Hall resistivity (ρ_{AHE}) and longitudinal resistivity (ρ_{xx}) for each mechanism: $\rho_{AHE} \propto \rho_{xx}^2$ for both the intrinsic and extrinsic side-jump mechanism, while $\rho_{AHE} \propto \rho_{xx}$ for extrinsic skew-scattering mechanism.

Experimentally, artificial impurities such as interfacial scattering in granular[8–10] and multilayer[11,12] films and surface scattering[13–15] have been applied to ferromagnetic materials both for the AHE mechanism exploration and magnetic sensor applications. However, the controversy over the effect of interface/surface scattering on the AHE remains. In granular thin films, interfacial scattering has been proved to dominate the AHE in Co-MgO system[10] but scattering-independent AHE has been reported in Fe-SiO_2 system.[9] In multilayer systems, both surface scattering dominated AHE[16] and interfacial scattering dominated AHE[17–20] have been reported,

[a]Author to whom correspondence should be addressed. Electronic mail: xixiang.zhang@kaust.edu.sa

which remains elusive. Furthermore, the interfacial scattering could also lead to other physical phenomenon such as giant magnetoresistance (GMR),[21,22] anisotropic magnetoresistance (AMR),[23] etc. Therefore, it is worth to study the interfacial scattering effect on the magneto-transport properties.

In our previous study, the interfacial scattering effect plays an important role in the AHE in Fe/Au[11] and Ni/Au[12] multilayers. Since the AHE and AMR both are related to the SOC and Au has relatively smaller SOC comparing to Ta, we then prepared Ta/Fe multilayers which have the same structure with that of Fe/Au multilayers[11] to study the interfacial scattering effect on the AMR and the AHE.

II. EXPERIMENTAL METHODS

$(\mathrm{Ta}_{\frac{12}{n}}/\mathrm{Fe}_{\frac{36}{n}})_n$ multilayers, where the numbers give the thickness in nanometer and n = 1, 2, 3, 4, 5, 6, 8, 10, 12, were prepared by sputtering system (Rotaris, Singulus). High purity targets, Fe (99.99%) and Ta (99.99%), were used for Fe and Ta layer deposition. The samples were deposited, at room temperature, on substrates of oxidized silicon wafers with the base pressure lower than 8.0×10^{-9} mbar. The deposition of 5 nm-thick SiO_2 as a top layer for each sample was to prevent sample oxidization. During deposition, the argon pressure was kept at 3×10^{-3} mbar. X-ray reflectivity (XRR) and high-angle θ–2θ measurements were carried out using x-ray diffraction (XRD) (D8 DISCOVERY, Bruker). The cross-section of samples was characterized by high-resolution scanning transmission electron microscopy (HR-STEM) (Titan 80-300, FEI) equipped with a spherical aberration corrector. The samples for magneto-transport measurements were patterned into Hall bars with dimensions 6.0 mm × 1.0 mm by mechanical masks. A five-contact geometry was used for simultaneously measuring the Hall resistivity and longitudinal resistivity on the same piece of sample by a physical property measurement system (Dynacool, Quantum Design).

III. RESULTS AND DISCUSSION

Figure 1(a) presents the temperature-dependent ρ_{xx} measured in a zero-magnetic field for all samples. All curves show a positive temperature coefficient of resistivity (TCR, $d\rho_{xx}/dT$), which suggests metallic electrical transport. Below 50 K, the ρ_{xx} shows very weak temperature dependence, indicating negligible contribution of photon scattering to the resistivity. With n increases from 1 to 12, the magnitude of ρ_{xx} shifts to higher values monotonically across the whole measured temperature range. This resistivity enhancement clearly indicates the increased scattering effect, including Ta/Fe interfacial scattering and grain boundary scattering within each layer. The Ta/Fe interfacial scattering plays much more important role in electrical properties than does grain boundary scattering due to the size effect, especially in samples with large n. To better demonstrate the interfacial scattering effect, Fig. 1(b) presents the ratio of $\rho_{xx}(n)/\rho_{xx}(n = 1)$ as a function of n at selected temperatures. The ratio

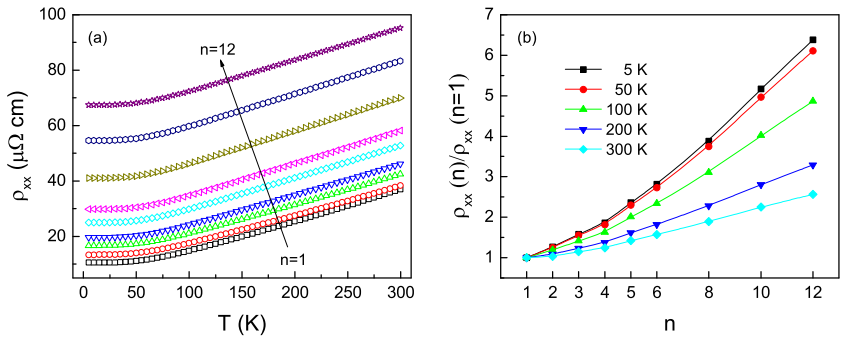

FIG. 1. (a) Temperature-dependent longitudinal resistivity for all samples; (b) $\rho_{xx}(n)/\rho_{xx}(n = 1)$ as a function of number of periods n for selected temperatures.

$\rho_{xx}(n = 12)/\rho_{xx}(n = 1)$ at 5 K is about 6.4 which is higher than that in Fe/Au multilayers,[11] being ascribed to the stronger interfacial scattering due to the rough interfaces including the intermixing of Ta and Fe at the interfaces, as shown in Fig. S2 of the supplementary material and corresponding analysis.

The interfacial scattering could also have crucial impact on magneto-transport properties. Spin-dependent interfacial scattering induced GMR has been reported in Fe/Cr multilayers.[21,22] Theoretical work has been reported that interfacial spin-orbit scattering could induce AMR.[23] In our previous work,[11] interfacial scattering resulted in AMR in Fe/Au multilayers due to the SOC of Au layers. Since the SOC is larger in Ta than that in Au, we then studied how the interfacial scattering affects the magnetoresistance. The magnetoresistance was measured with magnetic field in the film plane. With magnetic field parallel or perpendicular to the current, the MR ~ H curves were measured at 5 K for all samples. As seen in Fig. 2(a)–(i), AMR dominated the magneto-transport properties for all samples and minor GMR signals were shown in samples with n = 1–4 (see the detailed explanation about verifying the GMR and AMR behaviors in the supplementary material). The magnitude of AMR was plotted with n in Fig. 2(j). For comparison, the AMR values of the Fe/Au samples[11] were also plotted. The AMR value is defined as AMR = $\frac{R_{\parallel}(1000\,\mathrm{Oe})-R_{\perp}(1000\,\mathrm{Oe})}{R_{\perp}(1000\,\mathrm{Oe})}\times 100\%$, where $R_{\parallel}(1000\,\mathrm{Oe})[R_{\perp}(1000\,\mathrm{Oe})]$ is the resistivity when magnetic field parallel (perpendicular) to the measurement current at 1000 Oe. As seen in Fig. 2(j), the AMR increases with n in the Ta/Fe and Fe/Au samples. Since the AMR is caused by anisotropic scattering of carriers due to the SOC and is not related to the crystallinity of Fe layers, the enhancement of the AMR values from n = 1 to n = 12 could be ascribed to the interfacial

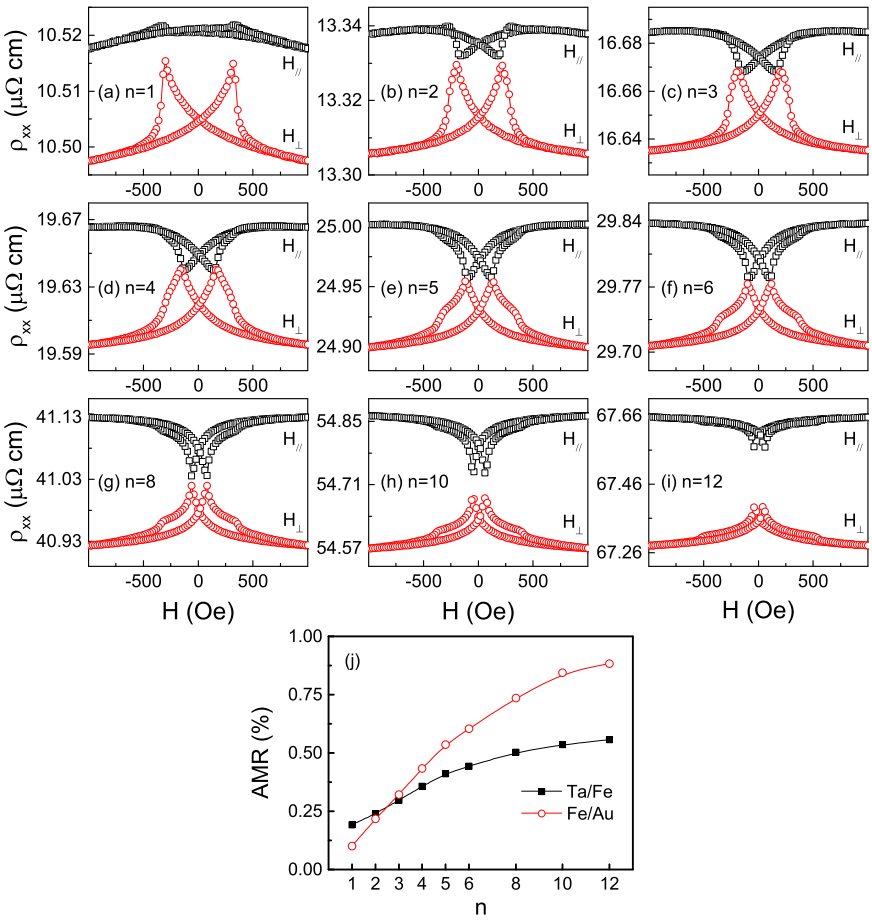

FIG. 2. (a)-(i) MR curves of all samples measured at 5 K. H$_{//}$($H_{\perp}$) indicates that the magnetic field was parallel (perpendicular) to the measurement current. The magnetic field swept from +1000 Oe to −1000 Oe and again to +1000 Oe. (j) the AMR values of Ta/Fe and Fe/Au multilayers as a function of n at 5 K.

spin-orbit scattering. However, we found that the AMR values increases more slowly in Ta/Fe multilayers with n than that in Fe/Au multilayers, although Ta has larger SOC than Au. The interfacial spin-orbit scattering does not only depend on the SOC but also depend on the quality of the interfaces between Fe and Ta(Au) layers. As analyzed in the STEM images of the multilayer cross-sections (Fig. S2 of the supplementary material), the interfaces between Ta and Fe are worse than that in Fe/Au samples. Therefore, the worse interfaces may suppress the spin-dependent scattering and affected the AMR values. Another phenomenon is that shoulders exist in the MR curves especially for the samples with n = 5−12. The shoulders may correspond to another magnetic phase which may be TaFe alloy (see Fig. S1(b) of the supplementary material and the corresponding analysis) because of the miscible property of the Ta and Fe layers. This is one more evidence to demonstrate the low quality of the Ta/Fe interfaces.

Figure 3(a) presents the field-dependent Hall resistivity (ρ_{xy}) measured with magnetic field perpendicular to the film plane at 5 K. Each curve shows a strong linear field dependence at low field until the magnetic saturation field (H_{sat}). Beyond the H_{sat}, the ρ_{xy} shows a much weaker linear field dependence. No coercivity was observed in all $\rho_{xy} \sim H$ hysteresis loops. These are the typical behaviors for ferromagnetic films with in-plane magnetic moments. To illustrate the temperature effect on the Hall resistivity, we measured the field-dependent ρ_{xy} of all samples at different temperatures (not shown). The curves at different temperatures show similar behaviors to that observed at 5 K. The ρ_{AHE} was extracted by extrapolating the ρ_{xy} data above the H_{sat} to zero field. Figure 3(b) shows the temperature-dependent ρ_{AHE} for all samples. The ρ_{AHE} increases with temperature for each sample, which shows the same tendency as the $\rho_{xx} \sim T$ curves. With n increases from 1 to 12, the ρ_{AHE} shifts to higher value in the full measured temperature range, which clearly demonstrates the interfacial scattering effect on the ρ_{AHE}.

We then start to analyze the mechanisms of the AHE. Recently, a new scaling relation,[24]

$$\rho_{\mathrm{AHE}} = \alpha\rho_{xx0} + \beta\rho_{xx0}^2 + b\rho_{xx}^2, \tag{1}$$

was proposed in Fe thin films, where α represents the contribution from the skew-scattering, β and b denote the side-jump and intrinsic anomalous Hall conductivity (AHC), respectively. The subscript '0' indicates that the data were measured at low temperatures where thermal effect is negligible. Here, we applied Eq. (1) to our data to obtain the contributions of skew-scattering, side-jump and intrinsic mechanism. At 5 K, Eq. (1) could be simplified to

$$\rho_{\mathrm{AHE0}}/\rho_{xx0} = \alpha + (\beta + b)\rho_{xx0} \tag{2}$$

by taking the approximations, $\rho_{\mathrm{AHE}}(5\ \mathrm{K}) \approx \rho_{\mathrm{AHE0}}$ and $\rho_{xx}(5\ \mathrm{K}) \approx \rho_{xx0}$. By plotting $\rho_{\mathrm{AHE0}}/\rho_{xx0}$ versus ρ_{xx0} and fitting this curve linearly, as shown in Fig. 4(a), the slope $\beta + b$ and intercept α were obtained. The obtained α value is $(1.24\pm0.51)\times10^{-3}$, which gives the skew-scattering contribution. By plotting the data, $\rho_{\mathrm{AHE}}(T)$ versus $\rho_{xx}^2(T)$ (not shown), of each sample and linearly fitting each curve, the slope b could be obtained. Taking the value of $\beta + b$ obtained in Fig. 4(a), the value of β could also be obtained. Figure 4(b) presents the values of b and β for all samples. As seen, the intrinsic

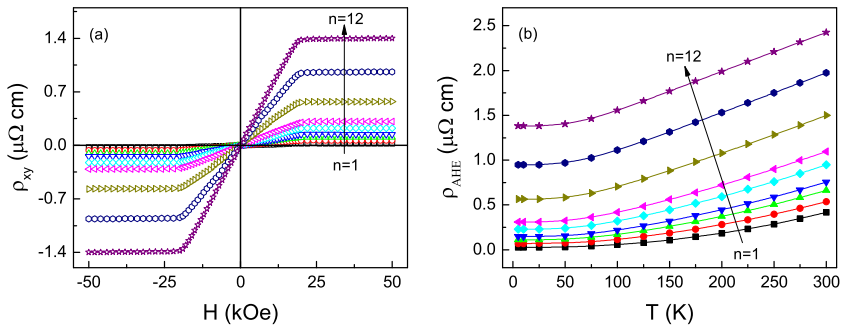

FIG. 3. (a) Field-dependent Hall resistivity of all samples at 5 K; (b) temperature-dependent anomalous Hall resistivity for all samples.

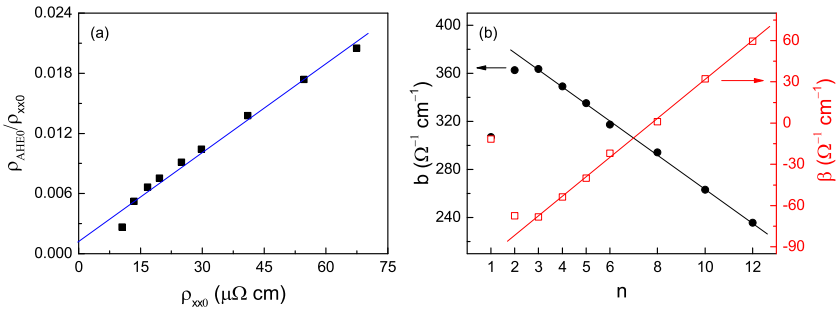

FIG. 4. (a) $\rho_{AHE0} \sim \rho_{xx0}$ curve measured at 5 K. The blue straight line is the least-squares fit to the data. (b) the values of b and β as a function of the number of period n. The solid lines are guides to eyes.

contribution decreases with n increases except the sample $n = 1$, which may be due to the crystallinity decaying or the finite size effect.[11,12,24,25] Remarkably, the sign of the side-jump contribution (β) changed from negative to positive with n increases from 1 to 12. The scattering-induced side-jump contribution may have two origins: interfacial scattering between Ta and Fe and grain boundary scattering inside each Fe layer. The two contributions to side-jump mechanism may have opposite signs, as reported in Co/Pd bilayers[26] and Ni/Au multilayers.[12] For samples with less periods, the grain boundary scattering induced side jump dominated, which give a negative β. As n increases, the interfacial scattering plays a more important role in side jump, which gives a positive β. As seen in Fig. 4(b), the intrinsic contribution is much larger than the side-jump contribution, showing an intrinsic mechanism-dominated AHE in Ta/Fe multilayers. This is consistent with the result in Fe/Au multilayers.[11] As seen in Fig. 4(a), ρ_{AHE0}/ρ_{xx0}, denoted as anomalous Hall angle, increases with n increases, which clearly suggests that the interfacial scattering enhanced the anomalous Hall angle. This enhancement may be of great benefit to the development of the AHE-based sensors.

IV. CONCLUSIONS

We prepared $(Ta_{\frac{12}{n}}/Fe_{\frac{36}{n}})_n$ multilayers and studied the interfacial scattering effect on the AMR and the AHE. The longitudinal resistivity increased by 6.4 times at 5 K from sample $n = 1$ to $n = 12$, indicative of the interfacial scattering effect. The interfacial spin-orbit scattering enhanced the AMR at 5 K. The enhancement of AMR is lower than that in Fe/Au multilayers[11] because of the rough interfaces and the intermixing of Ta/Fe, although the SOC of Ta is larger than that of Au. The skew-scattering, side-jump and intrinsic contributions to the AHE were separated successfully. As n increases from 1 to 12, the intrinsic contribution decreases because of the decaying crystallinity and finite size effect. The intrinsic contribution dominated the AHE for all samples, which is consistent with the result in Fe/Au multilayers.[11] The interfacial scattering and intralayer scattering both contribute to side jump in the AHE, but with opposite sign and, consequently, the overall side jump changes from negative to positive. The overall side jump shows the same tendency as that in Fe/Au multilayers.

SUPPLEMENTARY MATERIAL

See supplementary material for the structural characterization of the Ta/Fe multilayers and the verification of the GMR and AMR behaviors in the multilayers.

ACKNOWLEDGMENTS

The research reported in this publication was supported by funding from King Abdullah University of Science and Technology (KAUST). QZ and PL acknowledge the financial support by KAUST sensor project (REP/1/2708-01). XH acknowledges the financial support by KAUST sensor project (REP/1/2719-01).

[1] R. Karplus and J. M. Luttinger, Phys. Rev. **95**, 1154 (1954).
[2] J. W. Ye, Y. B. Kim, A. J. Millis, B. I. Shraiman, P. Majumdar, and Z. Tesanovic, Phys. Rev. Lett. **83**, 3737 (1999).
[3] T. Jungwirth, Q. Niu, and A. H. MacDonald, Phys. Rev. Lett. **88**, 207208 (2002).
[4] Y. G. Yao, L. Kleinman, A. H. MacDonald, J. Sinova, T. Jungwirth, D. S. Wang, E. G. Wang, and Q. Niu, Phys. Rev. Lett. **92**, 037204 (2004).
[5] J. Smit, Physica **21**, 877 (1955); **24**, 39 (1958).
[6] L. Berger, Phys. Rev. B **2**, 4559 (1970).
[7] N. Nagaosa, J. Sinova, S. Onoda, A. H. MacDonald, and N. P. Ong, Rev. Mod. Phys. **82**, 1539 (2010).
[8] A. B. Pakhomov, X. Yan, and B. Zhao, Appl. Phys. Lett. **67**, 3497 (1995).
[9] W. J. Xu, B. Zhang, Q. X. Wang, W. B. Mi, Z. Wang, W. Li, R. H. Yu, and X. X. Zhang, Phys. Rev. B **83**, 205311 (2011).
[10] Q. Zhang, Y. Wen, Y. L. Zhao, P. Li, X. He, J. L. Zhang, Y. He, Y. Peng, R. H. Yu, and X. X. Zhang, J. Phys.: Condens. Matter **29**, 415802 (2017).
[11] Q. Zhang, P. Li, Y. Wen, C. Zhao, J. W. Zhang, A. Manchon, W. B. Mi, Y. Peng, and X. X. Zhang, Phys. Rev. B **94**, 024428 (2016).
[12] Q. Zhang, P. Li, Y. Wen, X. He, Y. L. Zhao, J. L. Zhang, and X. X. Zhang, J. Phys. D: Appl. Phys. **50**, 235002 (2017).
[13] S. Sangiao, L. Morellon, G. Simon, J. M. De Teresa, J. A. Pardo, J. Arbiol, and M. R. Ibarra, Phys. Rev. B **79**, 014431 (2009).
[14] Z. B. Guo, W. B. Mi, Q. Zhang, B. Zhang, R. O. Aboljadayel, and X. X. Zhang, Solid State Commun. **152**, 220 (2012).
[15] L. Wu, K. Zhu, D. Yue, Y. Tian, and X. F. Jin, Phys. Rev. B **93**, 214418 (2016).
[16] O. Shaya, M. Karpovski, and A. Gerber, J. Appl. Phys. **102**, 043910 (2007).
[17] S. N. Song, C. Sellers, and J. B. Ketterson, Appl. Phys. Lett. **59**, 479 (1991).
[18] C. L. Canedy, X. W. Li, and G. Xiao, Phys. Rev. B **62**, 508 (2000).
[19] F. Zhang, F. S. Wen, Y. F. Lü, W. Li, Y. F. Lu, Z. Y. Liu, B. Xu, D. L. Yu, J. L. He, and Y. J. Tian, J. Appl. Phys. **110**, 033921 (2011).
[20] V. Keskin, B. Aktas, J. Schmalhorst, G. Reiss, H. Zhang, J. Weischenberg, and Y. Mokrousov, Appl. Phys. Lett. **102**, 022416 (2013).
[21] M. N. Baibich, J. M. Broto, A. Fert, F. Nguyen Van Dau, F. Petroff, P. Etienne, G. Creuzet, A. Friederich, and J. Chazelas, Phys. Rev. Lett. **61**, 2472 (1988).
[22] G. Binasch, P. Grünberg, F. Saurenhach, and W. Zinn, Phys. Rev. B **39**, 4828 (1988).
[23] S. S.-L. Zhang, G. Vignale, and S. F. Zhang, Phys. Rev. B **92**, 024412 (2015).
[24] Y. Tian, L. Ye, and X. F. Jin, Phys. Rev. Lett. **103**, 087206 (2009).
[25] L. Wu, K. Zhu, D. Yue, Y. Tian, and X. F. Jin, Phys. Rev. B **93**, 214418 (2016).
[26] X. L. Kou, J.-M. Schmalhorst, V. Keskin, and G. Reiss, J. Appl. Phys. **112**, 093915 (2012).